ELSEVIER

Biochimica et Biophysica Acta 1185 (1994) 177–187

BBA Biochimica et Biophysica Acta

Temperature-dependent electron spin polarization of the triplet state of the primary donor in *Rhodopseudomonas viridis*

J.S. van den Brink *, H. Manikowski [1], P. Gast, A.J. Hoff

Department of Biophysics, Huygens Laboratory, Leiden University, P.O. Box 9504, 2300 RA Leiden, The Netherlands

(Received 16 June 1993)

Abstract

The electron spin polarization (ESP) of the triplet of the primary donor (^{3}P) in reaction centers of the photosynthetic bacterium *Rhodopseudomonas viridis* shows an anisotropic temperature dependence (Van Wijk, F.G.H. and Schaafsma, T.J. (1988) Biochim. Biophys. Acta 936, 236). The reported inversion of the initial electron spin polarization (IESP) for the canonical *Y*-direction of ^{3}P at 100 K has been explained by means of coherent S-$T_{\pm}$ mixing in the radical pair, due to a fast relaxing electron spin on the iron-quinone acceptor complex X (Hore, P.J., Hunter, D.A., Van Wijk, F.G.H., Schaafsma, T.J. and Hoff, A.J. (1988) Biochim. Biophys. Acta 936, 249). Using direct-detection EPR, we show that at 100 K the IESP in randomly oriented samples is *not* inverted for the canonical *Y*-direction of ^{3}P. Furthermore, in single crystals the IESP at 100 K is shown to be almost zero for the complete *YZ*-plane of ^{3}P. Since $X^{\cdot -}$ shows a strong *g*-anisotropy, the model of Hore et al., in which polarization-inversion only occurs when the effective *g*-value of $X^{\cdot -}$ is around $g = 2.00$, is inadequate to explain the temperature-dependent changes of the IESP. Therefore, we conclude that anisotropic fast spin-lattice relaxation in the radical pair triplet state is the origin of the temperature dependence of the ESP. The inversion for the canonical *Y*-direction under continuous illumination is the result of the interplay of spin-lattice relaxation in ^{3}P and its triplet decay rates, in combination with changes in the IESP.

Key words: Photosynthesis; EPR; Electron spin polarization; Radical pair mechanism; Spin-lattice relaxation

1. Introduction

The primary events of electron transport in photosynthetic reaction centers (RCs) of purple bacteria are described by

$$PIX \xrightarrow{h\nu} P^*IX \rightarrow P^{\cdot +}I^{\cdot -}X \rightarrow P^{\cdot +}IX^{\cdot -} \quad (1)$$

where P denotes the primary electron donor, I the intermediary electron acceptor and X a complex of the primary quinone Q_A and a high-spin Fe^{2+} ($S = 2$) ion, which acts as the first (meta)stable electron acceptor. In *Rhodobacter (Rb.) sphaeroides* P is a bacteriochlorophyll *a* (BChl *a*) dimer, I a bacteriopheophytin *a* (BPh *a*) molecule, and Q_A a 1,4-benzoquinone derivative, UQ-10 [1]. The RC of *Rhodopseudomonas (Rps.) viridis* contains BChl *b* and BPh *b* instead of BChl *a* and BPh *a*, and Q_A is a 1,4-naphthoquinone derivative, MK-9 [2].

When forward electron transport is blocked by removal or reduction of Q_A, illumination produces the triplet state of the primary donor, ^{3}P:

$$PIX^- \xrightarrow{h\nu} P^*IX^{\cdot -} \rightarrow {}^1[P^{\cdot +}I^{\cdot -}]X^{\cdot -} \rightarrow {}^3[P^{\cdot +}I^{\cdot -}]X^{\cdot -} \rightarrow {}^3PIX^{\cdot -} \quad (2)$$

The conversion of the initial singlet state of the radical pair, $^1[P^{\cdot +}I^{\cdot -}]$, to its triplet state, $^3[P^{\cdot +}I^{\cdot -}]$, is driven by the difference in the local magnetic field and

* Corresponding author. Fax: +31 71 275815.

[1] Permanent address: Institute of Physics, Technical University, Poznan, Poland.

Abbreviations: RC, reaction center; BChl, bacteriochlorophyll; BPh, bacteriopheopytin; P, primary donor; I, intermediary acceptor, Q_A, first quinone acceptor; X, FeQ-complex; MK, menaquinone; UQ, ubiquinone; (I)ESP, (initial) electron spin polarization; EPR, electron paramagnetic resonance; *Rb., Rhodobacter*; *Rps., Rhodopseudomonas*; *A*, optical absorbance; A, absorption; E, emission; LDAO, lauryldimethylamineoxide; RYDMR, Reaction Yield Detected Magnetic Resonance.

SSDI 0005-2728(93)E0222-C

the electronic g-factor of the two radicals, and is influenced by magnetic dipolar and Heisenberg exchange interactions between the radicals. The yield of ^3P, ϕ_T, furthermore depends on the rates k_s and k_t with which the two radical pair states decay.

In the presence of a strong magnetic field B_0, the $T_\pm$ triplet sublevels are separated from the T_0 level by the Zeeman energy. Singlet-triplet conversion then takes place exclusively between the S and T_0 levels (energetically separated by J), thus reducing ϕ_T by about 50% at room temperature. From simulations of ϕ_T as a function of B_0, conclusions can be drawn on the characteristics of electron transport from P* to I, such as the functioning of the accessory BChl B_A, the change in free energy associated with the reaction steps, and the electronic coupling matrix elements (see, for example, [3–5]). In addition to its role in generating the magnetic field effect on ϕ_T, singlet-triplet conversion can produce electron spin polarization (ESP) in the radical pairs $P^{\cdot+}I^{\cdot-}$ and $P^{\cdot+}X^{\cdot-}$. Simulations of the resulting polarized EPR signals yield insight in the parameters governing electron transport [6–10].

The interpretation of magnetic field effects on reaction yields, and of the related effects of ESP, crucially depend on a detailed understanding of the mechanism of singlet-triplet conversion. Specifically, relaxation processes within the radical pair, or interactions with other paramagnetic species, will affect the validity of the conclusions drawn from simulations. Yet, very little is known on these processes. In this communication, we briefly review the theory of singlet-triplet conversion, the temperature dependence of the EPR signal of ^3P for RCs of *Rps. viridis* [11–14], and the models put forward for its explanation [13–16]. We show that the temperature-dependent inversion of the spin-polarization of the ^3P EPR signal of *Rps. viridis*, observed in single-crystals and solid solution in the temperature range 4–100 K, provides a unique opportunity to study the relaxation processes within the radical pair. We present new studies of the inversion phenomenon for RCs of *Rps. viridis* using cw and flash illumination, and cw and time-resolved direct-detection EPR. The results are compared with a previous study for *Rb. sphaeroides* [17], and are discussed in terms of the aforementioned models, using basic concepts of the theory of relaxation for a non-heme iron in a protein matrix [18]. We find that spin-lattice relaxation in the radical pair triplet state is significant and strongly anisotropic. The relaxation is most probably mediated by Heisenberg exchange between $I^{\cdot-}$ and $X^{\cdot-}$. This interaction is about two orders of magnitude larger in *Rps. viridis* than in *Rb. sphaeroides* [19,20], whence the triplet temperature dependence is much less pronounced in the latter species [12,17]. Some implications for the interpretation of magnetic field effects are discussed, and the major conclusions summarised. A preliminary account of this work has been presented at the 3rd International Workshop on Magnetic Resonance of Disordered Systems (EMARDIS 93) [21].

2. Theoretical considerations

The radical pair $P^{\cdot+}I^{\cdot-}$ is formed from P*I in a spin-correlated singlet state (Eq. 2). During the lifetime of the radical pair ($\approx$ 10 ns [22]), spin-rephasing in high magnetic fields, caused by hyperfine interactions (HFI) and the difference in g-values of $P^{\cdot+}$ and $I^{\cdot-}$, Δg, produces $^3[P^{\cdot+}I^{\cdot-}]$ exclusively in its T_0 state ($m_s = 0$), so-called S-T_0 mixing [6,7]. This two-spin model is valid for quinone-depleted RCs, and to first approximation also for native RCs of *Rb. sphaeroides*, in which the pre-reduced quinone radical is coupled very weakly with the primary radical pair: $J_{IX} \approx 0.1$ mT [20]. Because of the conservation of spin angular momentum, recombination from the radical pair produces ^3P in its T_0 state, excluding population of the $T_\pm$ sublevels ($m_s = \pm 1$). The $\Delta m_s = \pm 1$ EPR spectrum of ^3P then shows a characteristic AEEAAE electron spin polarization (ESP) pattern [23], where A and E denote enhanced absorption and emission, respectively. The ESP pattern is temperature dependent in RCs from *Rps. viridis*, changing from AEEAAE at 4 K to AEAEAE at about 25 K under steady-state illumination [12], and is reported to change to –EAEA– at 100 K immediately (3 μs) after laser excitation [13], where '–' means that no signal is observed. This temperature-dependent inversion phenomenon is absent in *Rb. sphaeroides* [12,17]. Since in *Rps. viridis*, in contrast to *Rb. sphaeroides*, $I^{\cdot-}$ is coupled strongly with $X^{\cdot-}$ by isotropic exchange interaction ($J_{IX} \approx 10$ mT [19]), a correlation between these two phenomena was proposed [12].

Two models have been put forward to explain this temperature-dependent polarization inversion in ^3P of *Rps. viridis*. In one model, the population of the $T_\pm$ sublevels of ^3P is explained by coherent S-$T_\pm$ mixing in the radical pair, due to exchange coupling with a third spin ($X^{\cdot-}$), which undergoes fast spin-lattice relaxation [15]. Inversion of the population of the triplet sublevels can be obtained for $g_{eff}(X^{\cdot-}) \approx 2.00$, provided the spin-lattice relaxation time T_1 of $X^{\cdot-}$ is less than 10 ns. This mechanism would explain the observed ESP pattern at higher temperatures, with the strong g-anisotropy of $X^{\cdot-}$ explaining the anisotropy of the temperature-dependent polarization inversion.

In the second model, fast relaxation in $^3[P^{\cdot+}I^{\cdot-}]$ induced by the fast relaxing $X^{\cdot-}$, is invoked to populate the $T_\pm$ levels [11]. Fig. 1 shows a schematic representation of this model, which has been modified slightly from Ref. 11 by deleting the thermal repopulation of $^3[P^{\cdot+}I^{\cdot-}]$, since this process does not occur for temper-

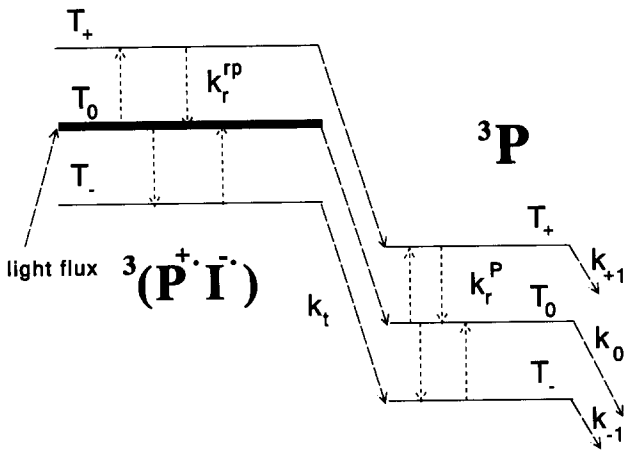

Fig. 1. Schematic representation of the states and kinetic pathways relevant for the description of the electron spin polarized ^{3}P signals in high B-field ($\approx$ 300 mT). $^3[P^{\cdot+}I^{\cdot-}]$ denotes the radical pair triplet state, which is assumed to be populated with 100% yield in the T_0 state after excitation of P. The spin-lattice relaxation rate of the radical pair triplet state is denoted with k_r^{rp}, while k_t denotes the decay rate from the sublevels of $^3[P^{\cdot+}I^{\cdot-}]$ to the corresponding sublevels of ^{3}P. k_r^P denotes the spin-lattice relaxation rate of ^{3}P. The sublevels of ^{3}P are depopulated with rate constants k_0 (for T_0) and $k_{\pm 1}$ (for $T_\pm$).

atures below 100 K [24]. In the case of fast relaxation in $^3[P^{\cdot+}I^{\cdot-}]$, it can be shown with the aid of Fig. 1 that (almost) exclusive S-T_0 spin interconversion in the radical pair, combined with spin-lattice relaxation in ^{3}P, explains the observed steady-state ESP pattern, AEAEAE. Note that by itself fast relaxation in the radical pair triplet can never give rise to *inversion* of the polarization. Equilibration of the triplet sublevels will be obtained if the spin-lattice relaxation rate of $^3[P^{\cdot+}I^{\cdot-}]$, k_r^{rp}, is larger than the decay rate from $^3[P^{\cdot+}I^{\cdot-}]$ to ^{3}P, k_t. The observation in Ref. 13 that at 100 K *initially*, i.e., before relaxation in ^{3}P takes place, the polarization of the EPR signal at the (low-field) canonical Y-direction appeared to be inverted, prompted therefore an extension of the model of Ref. 11, in which coherent S-$T_\pm$ mixing in the radical pair as in Ref. 15 explains the initial polarization inversion, and fast spin-lattice relaxation ($T_1 < 1$ ns) in $^3[P^{\cdot+}I^{\cdot-}]$, thermally repopulated from ^{3}P, explains the decay kinetics of the observed transients [13]. Unfortunately, this model did not demonstrate why relaxation in the original triplet radical pair state, which presumably is equally fast, is not equilibrating the three triplet sublevels, while there is no evidence that at $T \leq 100$ K activated repopulation of the radical pair occurs [24].

The polarization of ^{3}P was further investigated by Proskuryakov et al. [14], who obtained temperature-dependent EPR spectra of ^{3}P by the direct-detection method, using a boxcar integrator with signal integration over the first 10 μs after laser excitation. These spectra confirmed the unusual temperature dependence of the ESP (i.e., only the canonical X-direction is independent of temperature). However, no polarization inversion was observed for the canonical Y-direction up to 60 K. The anisotropic temperature-dependent changes of the ESP pattern were ascribed to anisotropic fast relaxation in the radical pair [16].

3. Materials and methods

Rps. viridis was grown anaerobically. RCs were isolated as described in [25], or by a somewhat faster method. Briefly, chromatophores ($A_{1060} = 40$ cm^{-1}) were incubated for 10 min at room temperature with 5% (w/v) LDAO in a Tris buffer, containing 10 mM Tris · HCl, 1 mM EDTA, at pH 8. Subsequently, the solution was centrifugated at 2000 × g for 5 min at 4°C, after which DEAE-Sephacel was added to the supernatant, and the mixture was incubated for a few minutes at 4°C, binding the RCs to the DEAE. The mixture was poured on a coarse glass-filter at room temperature and the DEAE was washed first with about the same volume of 5% (w/v) LDAO in Tris buffer as used for the incubation and, afterwards, with a quarter of the previously used volumes of 0.025% (w/v) LDAO in Tris buffer. The RCs were eluted using 0.2 M NaCl in 0.025% (w/v) LDAO in Tris buffer. The resulting RC-solution was dialysed overnight at 4°C against 0.05% (w/v) LDAO in Tris buffer. A value of 2.4 to 2.6 for the A_{280}/A_{830} ratio was routinely obtained, which compares quite well with the value of 2.3 using the method of Ref. 25. Additionally, the purity of the RCs was checked by means of SDS-PAGE, which yielded four subunit bands, identical to those obtained for RCs prepared according to Ref. 25.

A typical EPR sample had an A_{830} of 20 cm^{-1} and contained about 60 to 70% (v/v) glycerol. About 0.3 M sodium ascorbate was added to reduce the cytochromes, leaving the quinone neutral. The sample was frozen in the dark, such that no radicals were present in the RCs. Illumination at 4 K immediately produces the stable state $Cyt^{\cdot+}Q_A^{\cdot-}$.

EPR spectra were obtained using a Varian E-9 spectrometer equipped with a multi-purpose TE-101 cavity, which was modified for performing direct-detection measurements. The overall instrumental rise time was approx. 350 ns.

Single crystals of RCs were grown following the procedure described in Ref. 26. After soaking them in an imitation mother liquor containing 1.5 M sucrose, 2.5 M ammonium sulphate, 3% (w/v) heptanetriol, 0.1% (w/v) LDAO, 50 mM potassium phosphate (pH = 6) and a saturating amount of sodium ascorbate, the crystal was mounted on a quartz rod and frozen in the dark.

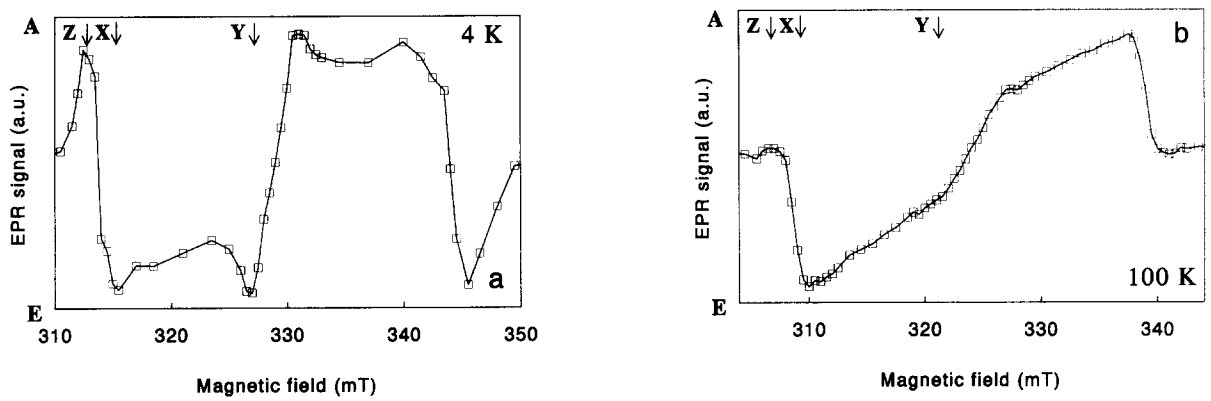

Fig. 2. Direct-detection EPR powder spectra of the initial electron spin polarized state of ^{3}P of *Rps. viridis* at 4 K (a) and 100 K (b). The points of the spectra are the average of ten points of the kinetic trace at the corresponding magnetic field value, for 10 ns intervals from 760 to 850 ns after excitation. Excitation wavelength, 852 nm; laser power, 10 mJ/pulse. (a). $T = 4$ K, microwave power, 0.2 mW; microwave frequency, 9.206 GHz. Each kinetic trace was averaged 400 times. (b). $T = 80$ K, microwave power, 1 mW; microwave frequency, 9.068 GHz. Each kinetic trace was averaged 900 times. Z, X and Y denote the transitions of the respective canonical directions of ^{3}P.

Light-modulated EPR spectra were obtained using an EG&G lock-in amplifier and an ILC 300 W Xe-lamp, whose intensity can be modulated with a frequency of up to 1 kHz.

For the laser flash-photolysis experiments, we used a tunable Ti-Sapphire laser, pumped with a Q-switched Nd-YAG laser (Continuum). The excitation wavelength was 852 nm. The absorption band of *Rps. viridis* at this wavelength is partly due to a higher exciton component of P [27,28], and bleaches completely on oxidation of P. Therefore, in the light pass of the laser pulse, all RCs will be excited using laser powers of typically 10–20 mJ/pulse. The pulse length was approx. 10 ns; the repetition rate was 10 Hz.

The kinetic traces were averaged using a LeCroy 9410 150 MHz digital oscilloscope equipped with signal-averaging facility, and were then stored in a personal computer for further analysis.

4. Results

The temperature dependence of the steady-state light-modulated EPR triplet spectrum of the primary donor in *Rps. viridis* is well known [12]. Fig. 2 shows direct-detection EPR spectra of ^{3}P at 4 and 100 K, obtained from the kinetics of the EPR signal for a randomly oriented sample. The spectrum is an average of ten points of the kinetic trace, from 760 to 850 ns after the exciting laser flash. Since the sampling time is relatively short compared with the decay times of the triplet sublevels (60 and 75 μs for X and Y, and 400 μs for Z [29]) and the spin-lattice relaxation in ^{3}P [13,17], we call this spectrum the Initial Electron Spin Polarized (IESP) EPR spectrum. It is clear from Fig. 2, that the initial population difference of the triplet sublevels for the canonical Y- and Z-directions is almost zero at 100 K. No initial polarization inversion is observed for these orientations.

For the low-field canonical Z-direction, the kinetic trace at 100 K is shown in Fig. 3. Using a two-component exponential fit, we obtain two decay rate constants, $(43 \pm 2) \cdot 10^3$ s^{-1} and $(12 \pm 2) \cdot 10^3$ s^{-1}, in good agreement with the data reported in Ref. 13. The kinetic trace was simulated in the framework of the model of Fig. 1, using equal initial population of the sublevels of ^{3}P, $k_{\pm 1} = 14.9 \cdot 10^3$ s^{-1}, $k_0 = 2.4 \cdot 10^3$ s^{-1} [29], and $k_r^P = 15 \cdot 10^3$ s^{-1}. The observed ratio of the *maximum* amplitude of the kinetic trace at 4 and 100 K, obtained with 40 μW microwave power, is about 6.

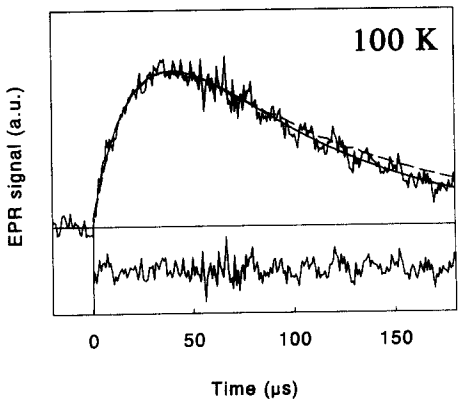

Fig. 3. Direct-detection EPR kinetic trace at 100 K for a frozen solution of RCs at the magnetic field value corresponding with the low-field canonical Z-direction of ^{3}P, as indicated in Fig. 2b. Microwave power, 1 mW; microwave frequency, 9.068 GHz; laser power, 10 mJ/pulse; excitation wavelength, 852 nm. The kinetic trace is the average of 900 transients. A two-exponential fit yields characteristic times of $\tau = 19$ μs for the growth of the signal, and $\tau = 79$ μs for its decay (solid line). The dotted line is a simulated trace obtained with the model of Fig. 1, and using the parameters mentioned in the text.

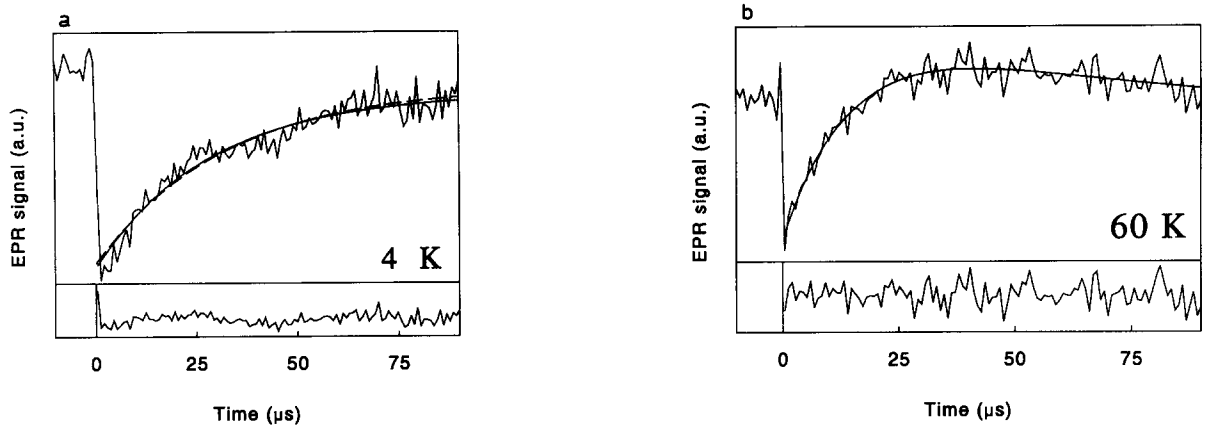

Fig. 4. Single-crystal direct-detection EPR kinetic traces at 4 K (a) and 60 K (b) for the specific case that $\boldsymbol{B}_0$ parallels the canonical Y-direction of ^{3}P for one of the magnetically non-equivalent sites of the crystal. Laser power, 10 mJ/pulse; excitation wavelength, 852 nm; 4900 transients were recorded at the low-field transition and averaged for each kinetic trace. (a). $T = 4$ K; microwave power, 50 μW; microwave frequency, 9.207 GHz. (b). $T = 60$ K; microwave power, 1 mW; microwave frequency, 9.208 GHz. At 60 K, the kinetic trace is initially emissive; after 20 μs a long-living absorptive component is observed. The solid line is the result of an exponential fit, the dashed line represents a simulated trace obtained with the model from Fig. 1, using rate constants mentioned in the text.

Using direct-detection EPR, it is not possible to obtain 'pure' traces for the other canonical directions, since in a random sample other orientations always contribute to the kinetics observed for the canonical X- and Y-direction. In RC single crystals, however, it indeed is possible to obtain kinetic traces with $\boldsymbol{B}_0$ parallel to one of the canonical directions [26]. In Fig. 4, kinetic traces at 4 and 60 K are shown for the specific crystal orientation and magnetic field value for which a transition at the canonical Y-direction is observed. This orientation is achieved when the crystal is rotated about 60° away from the specific orientation where all triplets overlap, rotating the crystal around the normal of the plane spanned by the crystal's long axis and the magnetic field direction [26]. Again, no initial inversion is observed; instead a clear emissive transient is found at the low-field transition. At 100 K, no signal could be observed, because of the poor signal-to-noise ratio of the kinetic trace when initially the three sublevels of ^{3}P are populated equally. The 4 K kinetic trace shows a single-exponential decay with $k = (35 \pm 2) \cdot 10^3$ s^{-1}, whereas the trace at 60 K is bi-exponential with rate constants of $(65 \pm 2) \cdot 10^3$ s^{-1} and $(18 \pm 2) \cdot 10^3$ s^{-1}. Simulations within the framework of the model of Fig. 1, using $k_0 = 16.1 \cdot 10^3$ s^{-1} and $k_{\pm 1} = 8.05 \cdot 10^3$ s^{-1}, yield for the 4 K kinetic trace: $[T_0]_{t=0} = 80\%$, $[T_+]_{t=0} = [T_-]_{t=0} = 10\%$, and $k_r^P = 5 \cdot 10^3$ s^{-1}. For the 60 K trace, we obtain: $[T_0]_{t=0} = 40\%$, $[T_+]_{t=0} = [T_-]_{t=0} = 30\%$, and $k_r^P = 30 \cdot 10^3$ s^{-1}.

Fig. 5 shows the light-modulated single-crystal EPR spectrum at 4 and 100 K for the same orientation as for the kinetic experiments. Now, polarization inver-

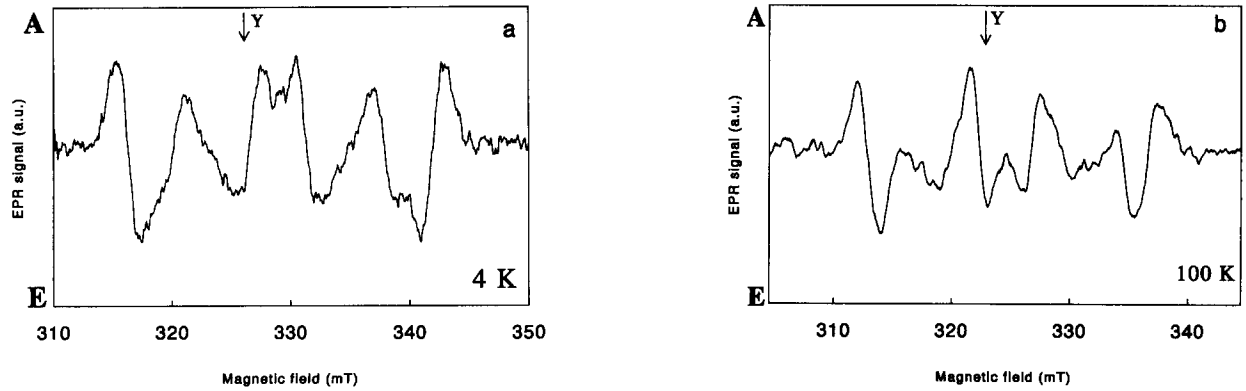

Fig. 5. Light-modulated single-crystal EPR spectra at 4 K (a) and 100 K (b), using 100 kHz magnetic field modulation. The crystal is oriented such that $\boldsymbol{B}_0$ is parallel to the canonical Y-direction for one of the magnetically non-equivalent sites [26]. The arrow indicates the magnetic field value for which the kinetic traces of Fig. 4 were obtained. It is evident that the observed ESP of ^{3}P in a single-crystal under continuous illumination changes sign at higher temperatures. Light modulation frequency, 483 Hz; microwave power, 10 mW; field modulation amplitude, 1.0 mT; scan time, 8 min. The spectrum is the average of 2 scans. (a). $T = 4$ K; time constant, 1 s; microwave frequency, 9.208 GHz. (b). $T = 100$ K; time constant, 3 s; microwave frequency, 9.068 GHz.

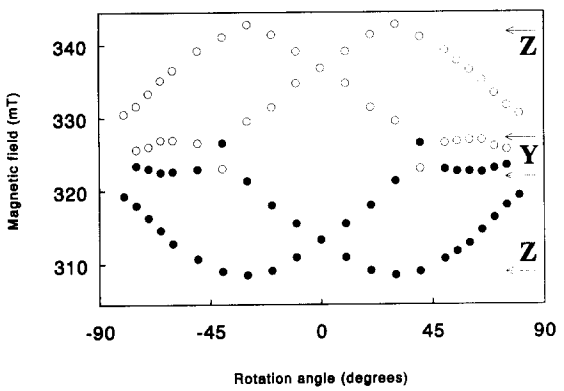

Fig. 6. The angle dependence at 100 K of the ^{3}P signals arising from the specific non-equivalent site within the single crystal for which $\boldsymbol{B}_0$ is rotated in the *ZY*-plane of ^{3}P. The crystal was rotated around one of its short axes. • denotes absorptive polarization, ○ denotes emissive polarization. Comparison with the corresponding figure in Ref. 26 shows that the polarization of ^{3}P is inverted for the canonical *Y*-direction of ^{3}P at 100 K.

sion indeed is observed for the canonical *Y*-direction. The angle dependence of the light-modulated ^{3}P EPR signals at 100 K is shown in Fig. 6 for that specific site in the unit cell for which the observed resonances shift between the canonical *Y*- and *Z*-direction [26]. For clarity, the resonances of the other three, magnetically inequivalent, sites are not shown. Comparing Fig. 6 with the angle dependence at 4 K reported in Ref. 26, it follows that the polarization inversion takes place over a rather broad range of angles, i.e., 45–90°. Furthermore, the kinetic trace for the canonical *Z*-direction in the single-crystal at 100 K is virtually identical to the one obtained in frozen solution (data not shown).

5. Discussion

The IESP EPR spectrum of ^{3}P in *Rps. viridis*, as shown in Fig. 2, is evidently different from that in *Rb. sphaeroides* R26 [17]. In this species, the features of all three canonical directions are visible at high temperatures, whereas in *Rps. viridis* only the signal related to the canonical *X*-axis of ^{3}P is present. The latter observation corroborates the data reported in Ref. 14. Our somewhat better resolution allows us to conclude that even at 100 K the initial polarization is still AEEAAE, although the amplitudes at the canonical *Y*- and *Z*-directions are very small.

Our direct-detection EPR data at 100 K contrast, however, with the kinetic traces for the canonical *Y*-direction shown in Ref. 13, which were obtained using 200 kHz magnetic-field modulation and a broadband pre-amplifier. The time resolution of this detection system was reported to be in the μs range [11]. The kinetics obtained at 17 and 40 K in Ref. 13 do not conflict with our single-crystal kinetic data obtained with direct-detection EPR, Fig. 4. At 100 K, however, a purely (enhanced) absorptive transition for the low-field *Y*-peak was reported in Ref. 13, whereas our measurements consistently show that for the canonical *Y*-direction no initial polarization inversion is present. The contrasting result of Ref. 13 may well be due to limitations of the 200 kHz field-modulation set-up. Since our data show that *initial* polarization inversion is absent at 100 K, we must reconsider the proposed models for the temperature dependence of the polarization.

For the discussion of the results of the flash experiments, the temperature dependence of the IESP and the kinetic behavior of ^{3}P can be treated seperately, since the lifetimes of $^3[P^{\cdot+}I^{\cdot-}]$ and of ^{3}P differ by about three orders of magnitude. Therefore, we will first discuss the temperature dependence of the spin dynamics in the radical pair, and afterwards that of the kinetics of ^{3}P.

Radical pair polarization

Considering the spin dynamics in the radical pair, two requirements should be met to explain a temperature-dependent change of the initial polarization of ^{3}P. First, there should be at least some population of the $T_{\pm}$ levels and second, this population must be anisotropic, because the polarization of the canonical *X*-direction is not affected by changing the temperature.

In the simulations of Hore et al. [15], the first requirement is met, since fast spin-lattice relaxation in $X^{\cdot-}$ induces S-$T_{\pm}$ mixing in the radical pair. The observed anisotropy of this effect is explained by the magnetic anisotropy of $X^{\cdot-}$, for which a very broad EPR spectrum is observed [30], whereas S-$T_{\pm}$ mixing is efficient only for a narrow range of values around $g_{\mathrm{eff}}(X^{\cdot-}) = 2.00$.

The angle dependence of the light-modulated EPR triplet spectra of single crystals at 100 K (Fig. 6) shows, however, that inversion does not occur in a *narrow* region of angles between the long axis of the crystal and $\boldsymbol{B}_0$, as one would expect from the strong *g*-anisotropy of $X^{\cdot-}$. Furthermore, the kinetic trace for the crystal orientation at which the molecules are oriented along the canonical *Z*-direction shows that the initial polarization is almost zero at 100 K (data comparable with Fig. 3, not shown). This implies that, at least for all orientations of $\boldsymbol{B}_0$ in the *YZ*-plane of ^{3}P, the T_0 and $T_{\pm}$ levels of $^3[P^{\cdot+}I^{\cdot-}]$ become equally populated during the lifetime of the radical pair. While rotating around the normal of the plane spanned by the crystal's long axis and $\boldsymbol{B}_0$, however, single-crystal EPR spectra of $X^{\cdot-}$ show a strong anisotropy [31,32] and no resonances are reported for $g_{\mathrm{eff}}(X^{\cdot-}) \approx 2.00$.

Combination of the above observations make it difficult to explain the angular dependence of the triplet signals at 100 K in terms of the model proposed by

Table 1
Angles between the magnetic axes of ^3P and $FeQ^{\cdot -}$, as defined in Refs. 31 and 41

	x_T	y_T	z_T
x_{FeQ}	72°	157°	76°
y_{FeQ}	109°	82°	20°
z_{FeQ}	153°	112°	104°

Hore et al. [15]. Considering the relative orientations of ^3P and $X^{\cdot -}$ (Table 1, see below), it is seen that the effective g-value of $X^{\cdot -}$ changes considerably while rotating the crystal in the YZ-plane of ^3P. Since the spin-exchange mechanism is effective only for a narrow field range (± 1.0 mT around $g = 2.00$, Fig. 3 in Ref. [15]), one would not expect population of $T_{\pm}$ for the observed broad angular range.

The IESP of ^3P at 100 K for the low-field peaks corresponding to the canonical Y- and Z-direction is still enhanced emissive and absorptive, respectively, albeit with very small amplitude (Fig. 2). It follows that the population of $T_{\pm}$ is indeed appreciable, approaching that of T_0, but that T_0 is still overpopulated. Therefore, the small population difference could be due exclusively to spin-lattice relaxation in $^3[P^{\cdot +}I^{\cdot -}]$. If this is the case, then the spin-lattice relaxation rate k_r^{rp} must be faster than the rate of decay from $^3[P^{\cdot +}I^{\cdot -}]$ to ^3P, k_t. For *Rps. viridis*, k_t is not available. Using the value for *Rb. sphaeroides*, $k_t = 4 \cdot 10^8$ s^{-1} [33], we obtain $k_r^{rp} > 10^9$ s^{-1} for temperatures above 25 K, the temperature at which the polarization changes sign under continuous illumination [12]. Since above 25 K the IESP for the canonical Z-direction still decreases with increasing temperature, k_r^{rp} must increase concomitantly. The inversion phenomenon is absent when the high-spin non-heme Fe^{2+} is either removed, or magnetically decoupled from the radical pair by double reduction of Q_A [12]. The latter observation also indicates that the presence of two oxidized cytochromes does not lead to relaxation enhancement in the radical pair. Corroborating evidence was obtained via measurements of the temperature dependence of the spin-lattice relaxation rate of $P^{\cdot +}$. If the cytochrome hemes are good relaxers of $P^{\cdot +}$, a distinct temperature dependence of T_1 would be expected. No such difference was observed, however, in comparing T_1 for $P^{\cdot +}$ of *Rps. viridis* and *Rb. sphaeroides* (Bosch, M.K. and Van den Brink, J.S., unpublished results). Therefore, the high-spin non-heme Fe^{2+}-ion seems to be the fast relaxer of the radical pair, acting via the exchange interaction between $I^{\cdot -}$ and $X^{\cdot -}$, J_{IX}.

To gain more insight in the role of the Fe^{2+}-ion in the induction of fast spin-lattice relaxation in $^3[P^{\cdot +}I^{\cdot -}]$, we consider some of the relevant aspects of the theory of spin-lattice relaxation for a Kramers' ion in a protein environment.

Spin-lattice relaxation of a Kramers' ion

The high-spin Fe^{2+}-ion of RCs cannot be observed with conventional X-band EPR, since the gap between the two lowest energy levels is approx. 140 GHz [30]. If Q_A is reduced, however, a broad X-band EPR spectrum is observed at cryogenic temperatures (< 20 K). This spectrum, attributed to a magnetically coupled complex of the Fe^{2+} and $Q_A^{\cdot -}$ complex, $X^{\cdot -}$, has been described theoretically for *Rb. sphaeroides* by Butler et al. [30]. The complex can be regarded as a Kramers' ion, for which only the two lowest doublet levels are populated at low temperature (4 K < T < 15 K). A general equation describing the temperature dependence of the spin-lattice relaxation of Kramers' ions is [18]:

$$\frac{1}{T_1} = aT + bT^n + c\Delta^3 e^{-\Delta/kT} \qquad (3)$$

where T_1 is the spin-lattice relaxation time, T the temperature, Δ the energy splitting between the two lowest Kramers' doublets, and a, b and c are phenomenological constants. The first term describes the direct relaxation process, in which the magnetic energy, $g\beta B_0$, of a spin flip of a paramagnetic ion is absorbed by a phonon of frequency ν_0. The last term describes the Orbach relaxation process, where a higher energy level is involved. These processes dominate at the lowest temperatures ($T < 4$ K). At higher temperatures ($T > 6$ K), T_1 is dominated by the Raman process (second term), in which an inelastic, two-phonon scattering process transforms the magnetic energy, $g\beta B_0$, of a spin flip of a paramagnetic ion into a change in lattice (that is, the RC-protein) vibrational energy of $h(\nu_1 - \nu_2)$. Stapleton and co-workers [34–36] correlated structural and relaxation properties of heme proteins and ferredoxins, which contain a low-spin Fe^{3+}, using the concept of a fractal dimensionality d of the protein. This dimensionality determines the temperature dependence of the spin-lattice relaxation of the Fe^{3+} Kramers' ion. The contribution of the Raman process varies with temperature as T^{3+2d}. For a regular three-dimensional lattice, $d = 2$, resulting in the well-known T^7 law for the temperature dependence of T_1.

The chain fractal dimension, d_c, of a biopolymer chain can be computed with a simple counting procedure [34]. The number of monomers N is determined as a function of radial distance R from an arbitrary origin, and the resulting function $N(R)$ is fitted to the function R^{d_c}. Using several origins, an accurate value for d_c is obtained. For proteins only the polypeptide backbone has to be considered, for which the C_α-atoms can be counted using the crystallographic coordinates from X-ray analysis. It has been found that d and d_c are identical for many globular, Fe^{3+}-containing proteins [35,36]. Since $X^{\cdot -}$ can be described as a Kramers'

ion [30], we expect that the fractal dimensionality concept of Stapleton et al. [34–36] is also valid for RCs.

The chain fractal dimension d_c for RCs of *Rps. viridis* was determined from the plot shown in Fig. 7a. Using the C_α-atoms of the amino-acids that coordinate with Fe^{2+} (His L190, L230, M217, M264, and Glu M232) or are close to Q_A (Thr M220 and Trp M250), we obtain $d_c = 1.26$ for $0.5 < R(\text{nm}) < 2.2$, and $N < 44$. Thus, we expect that T_1^{-1} is proportional to $T^{5.52}$ for $X^{\cdot-}$. Using the value of T_1 for *Rb. sphaeroides* at 4 K from Calvo et al. [37] as a reference, the expected temperature dependence of the spin-lattice relaxation rate of $X^{\cdot-}$ is shown in Fig. 7b. From calculations using the model of Fig. 1, with $k_0 = 16.1 \cdot 10^3\ s^{-1}$, $k_{\pm 1} = 8.05 \cdot 10^3\ s^{-1}$ [29], and $k_r^P = 20 \cdot 10^3\ s^{-1}$, it follows that the spin-lattice relaxation rate of the radical pair, k_r^{rp}, must be in the order of $10^9\ s^{-1}$ at 25 K to account for the observed polarization inversion under continuous illumination for the canonical *Y*-direction of ^3P. This agrees nicely with the spin-lattice relaxation rate of $X^{\cdot-}$ at 25 K obtained from the fractal model of Stapleton and co-workers (Fig. 7b).

Anisotropy of the inversion phenomenon

Since the IESP for the canonical *X*-direction of ^3P is, in contrast to that for the *Y*- and *Z*-directions, independent of temperature, we expect a large anisotropy for the Raman-type spin-lattice relaxation in both $^3[P^{\cdot+}I^{\cdot-}]$ and $X^{\cdot-}$. The magnetic interaction between the iron and the quinone anion radical is evidently anisotropic in *Rb. sphaeroides* [30], suggesting that the anisotropy of the temperature dependence of the IESP observed in *Rps. viridis*, could be due to such anisotropy. The three diagonal components of the magnetic interaction tensor, however, differ only by a factor of 4 [30]. Therefore, to explain the temperature *in*dependence of the IESP for the canonical *X*-direction of ^3P (which indicates that k_r^{rp} for the *X*-direction is more than three orders of magnitude less than that for the *Y*- and *Z*-directions), the spin-lattice relaxation of the Fe^{2+}-ion itself must be strongly anisotropic. The model of Stapleton et al. [34–36] may account for the anisotropy of the relaxation: Since a vibrational transition of the lattice should match the energy of a spin flip, $g\beta B_0$, isotropic spin-lattice relaxation in combination with the strong *g*-anisotropy of $X^{\cdot-}$ would require an isotropic distribution of lattice-vibrational modes. For Raman relaxation, this would imply an isotropic distribution of frequency differences $\Delta\nu$ for the two phonons involved in the spin flip. For the small globular protein BPTI (bovine pancreatic trypsin inhibitor) the distribution of low-frequency vibrational modes ($< 120\ cm^{-1}$) has been calculated [38]. Both the frequency and spatial distributions are evidently non-uniform, and, consequently, the distribution of $\Delta\nu$ will be anisotropic. Assuming that such a small protein can be regarded as a model for the RC-protein, the anisotropy of the phonon-distribution accounts for anisotropic relaxation of $X^{\cdot-}$, and thus for anisotropic relaxation in $^3[P^{\cdot+}I^{\cdot-}]$.

It follows from the combination of X-ray structural data [39,40] with single-crystal triplet [26,41] and $X^{\cdot-}$ [31,32] EPR data, that in *Rps. viridis* the canonical *X*-direction of ^3P coincides to within $\pm 10°$ with the *Z*-axis of the *g*-tensor of $X^{\cdot-}$ (Table 1). This direction is also nearly the direction of the approximate C_2-axis of the RC. Butler et al. [30] calculated that for the lowest two Kramers' doublets of $X^{\cdot-}$ the g_{zz}-values are 1.88 and 1.69. Evelo et al. [31] and Gast et al. [32] observed for single crystals of *Rps. viridis* at 4 K only EPR lines in the corresponding magnetic field range and assumed that severe line-broadening obscured

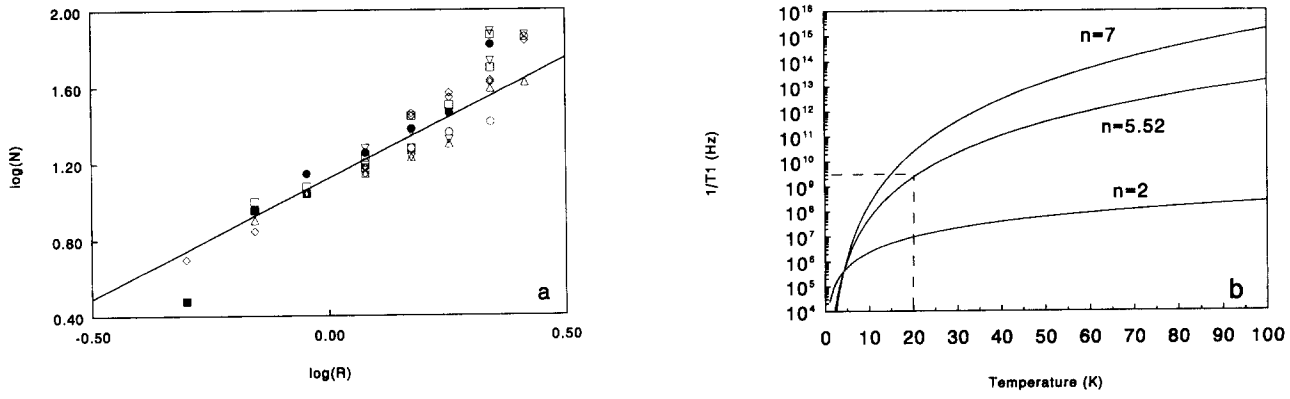

Fig. 7. (a). The number N of backbone-connected C_α-atoms within a sphere of radius *R* as a function of *R* for various origins of the sphere (different symbols), as indicated in the text. The C_α-atoms of the amino acids coordinating with Fe^{2+} and Q_A^- were used. The linear correlation between log(*N*) and log(*R*) for $0.5 < R(\text{nm}) < 2.2$ and $N < 44$ leads to a chain fractal dimension d_c of 1.26. (b). Predicted temperature dependence of the spin-lattice relaxation rate of $X^{\cdot-}$, using $T_1 \propto T^n$. As a reference, the value for *Rb. sphaeroides* at $T = 4$ K from Ref. 37 was taken. $n = 7$ for a non-Kramers' salt, $n = 2$ for a system with phonon bottleneck, and $n = 5.52$ within the fractal model. It is seen that in the last case the predicted spin-lattice relaxation rate for 25 K is in the expected range, viz. $\sim 10^9\ s^{-1}$ [13].

other resonances. This corroborates our hypothesis of anisotropic T_1 if the crystallographic axes, to which the rotational degrees of freedom in our experimental set-up are constricted, are close to the axes of the ***g***- or ***D***-tensor. Although this is apparently the case for the ***D***-tensor of ^{3}P [26], and inspection of the relative orientation of the ***g***-tensor of $X^{\cdot -}$ with respect to that of the dipolar tensor of ^{3}P [41] shows that the directions of their principal axes are similar to within $\pm 10°$, a full determination of the angular dependence of the EPR spectrum and the spin-lattice relaxation rate of $X^{\cdot -}$ in a single crystal is necessary to confirm our hypothesis that anisotropic spin-lattice relaxation of $X^{\cdot -}$ is responsible for the temperature-dependent changes in ESP of ^{3}P.

Comparison with Rb. sphaeroides

The direct-detection EPR spectra of ^{3}P for *Rb. sphaeroides* [17] indicate that in this bacterium the IESP of ^{3}P is normal, i.e., AEEAAE, up to room temperature. Assuming that fast spin-lattice relaxation in $^3[P^{\cdot +}I^{\cdot -}]$ indeed causes the temperature dependence of the IESP in *Rps. viridis*, it follows from the temperature *in*dependence in *Rb. sphaeroides* that $k_r^{rp} \ll k_t$ in that species. Hence, for *Rps. viridis* k_r^{rp} should be $> 10^9$ s^{-1}, whereas for *Rb. sphaeroides* k_r^{rp} should be $< 10^7$ s^{-1}, even at room temperature. A difference in dipolar coupling between $X^{\cdot -}$ and $I^{\cdot -}$ cannot contribute much to the observed difference in IESP, since their mutual distance is almost equal for both species. The magnitude of J_{IX} differs significantly in the two bacteria, being approx. 0.1 and 10 mT [19,20]. When the spin-lattice relaxation rate of $^3[P^{\cdot +}I^{\cdot -}]$ is proportional to J_{IX}^2 [42–44], it is about 10^4 times smaller in *Rb. sphaeroides* than in *Rps. viridis*. This difference between the k_r^{rp} values of the two species may explain the fact that for *Rb. sphaeroides* the IESP is normal up to room temperature (i.e., $k_r^{rp} < 10^7$ s^{-1}).

In principle, also J_{QFe} may be different for both bacteria, because of the presence of a different type of quinone in the bacteria, i.e., a benzoquinone (UQ-10) in *Rb. sphaeroides* and a naphthoquinone (MK-9) in *Rps. viridis*. The implications of this difference in quinones have not yet been studied thoroughly. Nevertheless, since the gross features of the EPR spectrum of $X^{\cdot -}$ are not very different for both species, we expect that J_{QFe} does not differ much. We conclude therefore that the difference in J_{IX} is the origin of the difference in temperature dependence of the IESP in *Rps. viridis* and *Rb. sphaeroides*.

Magnetic field effects

Most investigations of the influence of a magnetic field on the physical parameters of the radical pair mechanism and on ϕ_T are performed with quinone-depleted RCs of *Rb. sphaeroides* R26. In this system, an isolated radical pair is observed, such that $k_r^{rp} \ll k_t$. The presence of a quinone-anion radical complicates the interpretation of the magnetic field effects, as relative changes in the energy levels of the radical pair states may result from the presence of additional magnetic and electrostatic interactions. In the presence of the reduced iron-quinone complex, a broadened RYDMR signal is observed [45], which has been interpreted in terms of life-time broadening of the radical pair. Magnetic exchange interactions, *g*-value differences, and electronic dipolar terms have been shown to have a pronounced effect on simulations of magnetic field effects [46,47].

The effects of fast spin-lattice relaxation in $^3[P^{\cdot +}I^{\cdot -}]$ reported in this work, further complicates the interpretation of magnetic field effects in three-spin systems. We expect, for example, that in studies of ϕ_T as a function of B_0, an increase of temperature will obscure the so-called $2J$-resonance, due to relaxation-induced population of the $T_\pm$ sublevels of the radical pair, resulting in an increase of ϕ_T at high magnetic fields. A relevant experiment to check this hypothesis would be the measurement of the temperature dependence of ϕ_T at 0.1 T. Furthermore, RYDMR experiments may allow to discriminate between the coherent spin-exchange model of Ref. 15 and the incoherent process of spin-lattice relaxation in the radical pair [45].

Kinetics of ^{3}P

We now consider the temperature dependence of the kinetics of ^{3}P. Optical measurements of the temperature dependence of the average lifetime of ^{3}P in *Rb. sphaeroides* [24] and in *Rps. viridis* (E.M. Franken and J.S. van den Brink, unpublished results) indicate that at zero field the average triplet lifetime is constant between 4 and 100 K. It follows that the sublevel decay rates of the molecular triplet are largely temperature independent. These data also show that thermal repopulation of the radical pair from ^{3}P does not occur below 100 K. Therefore, the temperature dependence of the spin-lattice relaxation rates of ^{3}P, together with changes of the initial populations of the triplet sublevels, must explain the observed changes in lifetime observed with EPR [13].

Our direct-detection EPR measurements of the temperature dependence of the kinetic traces of ^{3}P are consistent with the data obtained by Van Wijk [13], except for the single-exponential rate constant for the canonical *Y*-direction at 4 K. Our direct-detection kinetic traces, however, are more informative than the kinetic traces obtained with magnetic field modulation in Ref. 13, since absolute amplitudes can be compared. We have compared the amplitudes of the kinetic traces for the canonical *Z*-direction at different temperatures, using a microwave power which is non-saturating

at 4 K, viz. 40 μW. Since we know that the IESP is almost zero at 100 K, we can calculate from the model of Fig. 1 the ratio of *maximum* amplitudes of the kinetic traces at 4 and 100 K, assuming exclusive T_0-population at 4 K, and using the triplet decay rates from Ref. 29 and the spin-lattice relaxation rates from Ref. 13. This ratio approximates 22, contrasting our measured ratio of 6. Although we cannot exclude the possibility of an increase of the triplet yield at 330 mT between 4 and 100 K, induced by opening of the $T_{\pm}$ populating channels at higher temperatures, it is unlikely that it will increase with a factor of 3 to 4. This argument, together with the kinetic data obtained for the *Y*-peak at 4 K, leads to the conclusion that even at 4 K there is some population of the $T_{\pm}$ levels (±20%). Using a reasonable value for k_r^{rp} at 4 K ($k_r^{rp} = k_r^{X} \approx 10^6$ s^{-1} [37]), it can be shown that such a population of $T_{\pm}$ can easily be achieved by anisotropic spin-lattice relaxation in $^3[P^{\cdot+}I^{\cdot-}]$, with a rate comparable to that in $X^{\cdot-}$. Simulations show that a small population of $T_{\pm}$ (up to ±20%) is difficult to determine in the kinetic traces. Although the initial decay is evidently not mono-exponential, no initial signal increase is observed within the signal-to-noise ratio. Thus, our experiments do not exclude up to 20% initial $T_{\pm}$ population of ^3P at 4 K. This is consistent with the fact that for the canonical *Y*-direction the decay rate constant obtained from the fit of the kinetic trace in Fig. 4a differs from k_0.

The kinetic traces for the canonical *Y*-direction in the single crystal, obtained with direct-detection EPR at 4 and 60 K (Fig. 4), are in agreement with its steady-state ESP shown in Fig. 5. Although the IESP is evidently emissive at 60 K, also a long-lived absorptive component is observed in the kinetic trace. This component can be simulated using the rate constants from Refs. 13 and 29. A simulation using steady-state illumination conditions results in an enhanced absorptive signal, in agreement with our observations. At 100 K, and using single-crystal direct-detection EPR experiments, we were not able to observe a kinetic trace for the canonical *Y*-direction of ^3P. When $[T_0]_{t=0} = [T_{\pm}]_{t=0} = 0.33$, the calculated amplitude of this kinetic trace is indeed very small and not detectable, given our signal-to-noise ratio. Nevertheless, the calculated amplitude of the *Y*-peak under *continuous* illumination at 100 K is only three times smaller than for the *Z*- and the *X*-directions, in agreement with experimental observations [12].

6. Conclusions

The IESP of ^3P in *Rps. viridis* shows an anisotropic temperature dependence. From single-crystal results, we conclude that the three-spin model of Hore et al. [15] is inadequate to explain the temperature dependence of the IESP. The disappearance of the spectral features for the canonical *Y*- and *Z*-directions in the IESP spectrum are explained with fast anisotropic spin-lattice relaxation in $^3[P^{\cdot+}I^{\cdot-}]$ ($k_r^{rp} > 10^9$ s^{-1} for $T > 25$ K). The observed inversion of the *Y*-peak of ^3P under continuous illumination is explained by the temperature dependence of the IESP taking into account the relative magnitudes of k_r^P and the ^3P sublevel-decay rate constants.

The relaxation in $^3[P^{\cdot+}I^{\cdot-}]$ is enhanced by relaxation in $X^{\cdot-}$. The temperature dependence of the spin-lattice relaxation rate of the latter apparently follows the T^{3+2d} relationship proposed by Stapleton and co-workers [34–36] in the framework of the fractal dimensionality model for Raman-type relaxation of a Kramers' ion in a protein matrix. The anisotropy of the temperature dependence of the IESP indicates that vibrations of the crystal field of the Fe^{2+}-ion impose an anisotropic phonon distribution on the RC protein.

7. Acknowledgements

The authors thank Dr. P.J. Hore (Physical Chemistry Laboratory, Oxford University, UK) for helpful discussions. Ms. S.J. Jansen is acknowledged for help with preparing the RCs, and Mr. R.J. Hulsebosch for taking part in some of the experiments. This work was supported by the Netherlands Foundation for Chemical Research (SON), financed by the Netherlands Organization for Scientific Research (NWO), and by Twinning Grant no. SC1*-CT90-0569 of the European Community. P.G. is a research fellow of the Royal Netherlands Academy of Arts and Sciences (KNAW). H.M. acknowledges the financial support of the Netherlands Ministry of Education during his stay in Leiden.

8. References

[1] Hiraishi, A. and Hoshino, Y. (1984) J. Gen. Appl. Microbiol. 30, 435–448.
[2] Shopes, R.J. and Wraight, C.A. (1985) Biochim. Biophys. Acta 806, 348–356.
[3] Lersch, W. and Michel-Beyerle, M.E. (1987) Biochim. Biophys. Acta 891, 265–274.
[4] Ogrodnik, A., Volk, M., Letterer, R., Feick, R. and Michel-Beyerle, M.E. (1988) Biochim. Biophys. Acta 936, 361–367.
[5] Goldstein, R.A. and Boxer, S.G. (1989) Biochim. Biophys. Acta 977, 78–86.
[6] Levanon, H. and Norris, J.R. (1978) Chem. Rev. 78, 185–198.
[7] Hoff, A.J. (1984) Q. Rev. Biophys. 17, 153–182.
[8] Mclauchlan, K.A. (1990) in Advanced EPR, Applications in Biology and Biochemistry (Hoff, A.J., ed.), pp. 345–368, Elsevier, Amsterdam.

[9] Stehlik, D., Bock, C.H. and Thurnauer, M.C. (1990) in Advanced EPR, Applications in Biology and Biochemistry (A.J. Hoff, ed.), pp. 371–402, Elsevier, Amsterdam.
[10] Hore, P.J. (1990) in Advanced EPR, Applications in Biology and Biochemistry (A.J. Hoff, ed.), pp. 405–438, Elsevier, Amsterdam.
[11] Van Wijk, F.G.H. (1987) Dissertation, Agricultural University Wageningen.
[12] Van Wijk, F.G.H., Gast, P. and Schaafsma, T.J. (1988) Photobiochem. Photobiophys. 11, 95–100.
[13] Van Wijk, F.G.H. and Schaafsma, T.J. (1988) Biochim. Biophys. Acta 936, 236–248.
[14] Proskuryakov, I.I., Shkuropatov, A.Y., Voznyak, V.M. and Shuvalov, V.A. (1988) Biofizika 33, 877–879.
[15] Hore, P.J., Hunter, D.A., Van Wijk, F.G.H., Schaafsma, T.J. and Hoff, A.J. (1988) Biochim. Biophys. Acta 936, 249–258.
[16] Manikowski, H. and Proskuryakov, I.I. (1993) Curr. Top. Biophys. 16, 53–56.
[17] Hoff, A.J. and Proskuryakov, I.I. (1985) Chem. Phys. Lett. 115, 303–310.
[18] Pilbrow, J.R. (1990) Transition Ion Electron Paramagnetic Resonance, Oxford University Press, Oxford.
[19] Prince, R.C., Tiede, D.M., Thornber, J.P. and Dutton, P.L. (1977) Biochim. Biophys. Acta 462, 467–490.
[20] Okamura, M.Y., Isaacson, R.A. and Feher, G. (1979) Biochim. Biophys. Acta 546, 394–417.
[21] Van den Brink, J.S., Manikowski, H., Gast, P. and Hoff, A.J., Appl. Magn. Res., in the press.
[22] Holten, D., Windsor, M.W., Parson, W.W. and Thornber, J.P. (1978) Biochim. Biophys. Acta 501, 112–126.
[23] Dutton, P.L., Leigh, J.S. and Seibert, M. (1972) Biochem. Biophys. Res. Commun. 46, 406–413.
[24] Chidsey, C.E.D., Takiff, L., Goldstein, R.A. and Boxer, S.G. (1985) Proc. Natl. Acad. Sci. USA 82, 6850–6854.
[25] Den Blanken, H.J. and Hoff, A.J. (1982) Biochim. Biophys. Acta 681, 365–374.
[26] Gast, P., Wasielewski, M.R., Schiffer, M. and Norris, J.R. (1983) Nature (London) 305, 451–452.
[27] Vermeglio, A. and Paillotin, G. (1982) Biochim. Biophys. Acta 681, 32–40.
[28] Vrieze, J. and Hoff, A.J. (1990) in Reaction Centers of Photosynthetic Bacteria (Michel-Beyerle, M.E., ed.), pp. 409–422, Springer, Berlin.
[29] Den Blanken, H.J., Jongenelis, A.P.J.M. and Hoff, A.J. (1983) Biochim. Biophys. Acta 725, 472–482.
[30] Butler, W.F., Calvo, R., Fredkin, D.R., Isaacson, R.A., Okamura, M.Y. and Feher, G. (1984) Biophys. J. 45, 947–973.
[31] Evelo, R.G., Nan, H.M. and Hoff, A.J. (1988) FEBS Lett. 239, 351–357.
[32] Gast, P., Gottschalk, A., Norris, J.R. and Closs, G.L. (1989) FEBS Lett. 243, 1–4.
[33] Goldstein, R.A. and Boxer, S.G. (1989) Biochim. Biophys. Acta 977, 70–77.
[34] Allen, J.P., Colvin, J.T., Stinsson, D.G., Flynn, C.P. and Stapleton, H.J. (1982) Biophys. J. 38, 299–310.
[35] Colvin, J.T. and Stapleton, H.J. (1985) J. Chem. Phys. 82, 4699–4706.
[36] Wagner, G.C., Colvin, J.T., Allen, J.P. and Stapleton, H.J. (1985) J. Am. Chem. Soc. 107, 5589–5594.
[37] Calvo, R., Butler, W.F., Isaacson, R.A., Okamura, M.Y., Fredkin, D.R. and Feher, G. (1982) Biophys. J. 37, 111a.
[38] Go, N., Noguti, T. and Nishikawa, T. (1983) Proc. Natl. Acad. Sci. USA 80, 3696–3700.
[39] Deisenhofer, J., Epp, O., Miki, K., Huber, R. and Michel, H. (1984) J. Mol. Biol. 180, 385–395.
[40] Deisenhofer, J., Epp, O., Miki, K., Huber, R. and Michel, H. (1984) Nature (London) 318, 618–624.
[41] Norris, J.R., Budil, D.E., Gast, P., Chang, C.-H., El-Kabbani, O. and M. Schiffer (1989) Proc. Natl. Acad. Sci. USA 86, 4335–4339.
[42] Solomon, I. (1955) Phys. Rev. 99, 559–565.
[43] Abragam, A. (1961) The Principles of Nuclear Magnetism, Clarendon Press, Oxford.
[44] Hirsh, D.J., Beck, W.F., Innes, J.B. and Brudvig, G.W. (1992) Biochemistry 32, 532–541.
[45] Budil, D. (1986) Ph.D. Thesis, University of Chicago.
[46] Hoff, A.J. (1981) Q. Rev. Biophys. 14, 599–665.
[47] Boxer, S.G., Chidsey, C.E.D., Roelofs, M.G. (1982) Proc. Natl. Acad. Sci. USA 79, 4632–4636.